American Mineralogist, Volume 95, pages 1413–1421, 2010

Crystal chemistry and low-temperature behavior of datolite: A single-crystal X-ray diffraction study

ROMANO RINALDI,[1] G. DIEGO GATTA,[2,3,*] AND ROSS J. ANGEL[4]

[1]Dipartimento di Scienze della Terra, Università degli Studi di Perugia, Piazza Università 1, I-06100 Perugia, Italy
[2]Dipartimento di Scienze della Terra, Università degli Studi di Milano, Via Botticelli 23, I-20133 Milano, Italy
[3]CNR-Istituto per la Dinamica dei Processi Ambientali, Via Mario Bianco 9, 1-20131 Milano, Italy
[4]Crystallography Laboratory, Department of Geosciences, Virginia Polytechnic Institute and State University, Blacksburg, Virginia 24060, U.S.A.

ABSTRACT

The crystal chemistry of six natural datolites from different localities was investigated by electron microprobe analysis in the wavelength dispersive mode and single-crystal X-ray diffraction. The chemical analyses show no significant site substitution. The single-crystal structure refinements confirm the structural model of datolite previously reported (with $a \sim 4.83$, $b \sim 7.61$, $c \sim 9.63$ Å, and $\beta \sim 90.15°$, space group $P2_1/c$). Intra-polyhedral bond distances and angles show common features in all samples at room T: (1) the Si-tetrahedron is strongly deformed, with Si-O distances ranging between ~1.57 and ~1.66 Å and O-Si-O angles ranging between ~105.4 and ~115.3°; (2) the B-tetrahedron is almost regular; (3) the Ca-polyhedron is significantly distorted, with bond distances ranging between ~2.28 and ~2.67 Å; (4) only one independent H-site occurs and its refined position suggests a bifurcated hydrogen bonding scheme with O5 as donor and O4 and O2 as acceptors [with O5-H ~ 0.8 Å and (1) O5···O4 ~ 2.99 Å, H···O4 ~ 2.33 Å, and O5-H···O4 ~ 140°, and (2) O5···O2 ~ 2.96 Å, H···O2 ~ 2.36 Å, and O5-H···O2 ~ 131°]. Low-temperature diffraction measurements between 300 and 100 K show that the thermal expansion of datolite is mainly governed by the axial response along [100] and [010], whereas the c-axis length is almost unchanged in this temperature interval. The volume thermal expansion coefficient ($\alpha_V = V^{-1}\partial V/\partial T$) between 100 and 280 K is $\alpha_V = 1.5(2)\cdot 10^{-5}$ K^{-1}. The higher thermal expansion of the a-axis is due to the layered nature of the structure of datolite: the Ca-O bond distances are the most compressible and expandable, and govern the contraction, upon cooling, along the direction perpendicular to the polyhedral layers. The tetrahedral layer is significantly more rigid and no changes of the tetrahedral tilts are observed from 300 to 100 K.

Keywords: Datolite, crystal structure, crystal chemistry, low temperature, single-crystal X-ray diffraction

INTRODUCTION

Datolite, a calcium boron hydroxide nesosilicate with ideal formula $CaBSiO_4(OH)$, has several interesting features that have been the subject of several crystallographic and mineralogical studies, since its first structural determination by Ito and Mori (1953). Following this early work, which was impaired by the inadequacy of the methods at that time, a series of structural reinvestigations (e.g., Pant and Cruickshank 1967; Foit et al. 1973; Bellatreccia et al. 2006; Ivanov and Belokoneva 2007) were aimed at improving the determinations of the Si-O and B-O bond lengths and bonding scheme. Foit et al. (1973) resolved many of these details, including the location of the hydrogen atoms. Recent structural studies have clarified the crystal-chemical relationships of datolite with the rare mineral okayamalite [$Ca_2SiB_2O_7$, Olmi et al. (2000)] and with the newly re-examined structure of bakerite [$Ca_4B_5Si_3O_{15}(OH)_5$, Perchiazzi et al. (2004)]. More recently, a study of the electron density provided a basis for the quantitative characterization of the bonded interactions in datolite (Ivanov and Belokoneva 2007); it showed that closed-shell type interactions exist between Ca and O atoms, whereas the Si-O and B-O bonds exhibit an intermediate nature with a strong covalent component. The bonded interactions in many mineral structures, including datolite, were recently reviewed by Gibbs et al. (2008).

Datolite has a layered structure (Fig. 1) with two sets of layers alternating along the [100] axis; the first is made up of alternating SiO_4 and BO_4 corner-sharing tetrahedra arranged in 8- and 4-membered rings, while the second layer consists of 8-coordinated Ca polyhedra arranged in 6-membered rings. Despite its apparent structural simplicity, the details of bonding interactions involving the light atoms B and H represent a challenge for X-ray structure determinations of this mineral.

One of the applications of datolite is as a geochemical marker, as shown by Bellatreccia et al. (2006) for datolites found in volcanic ejecta in Central Italy, and by Zaccarini et al. (2008) for datolites in ophiolitic basalts of the Northern Italian Apennines. The interest in datolite also rests on its technological applications in the glass and ceramic industries for electrical engineering (Konerskaya et al. 1988; Podlesov et al. 1992), membrane technology (Farsiyants et al. 1989; Schubert 2003), as well as in

* E-mail: diego.gatta@unimi.it

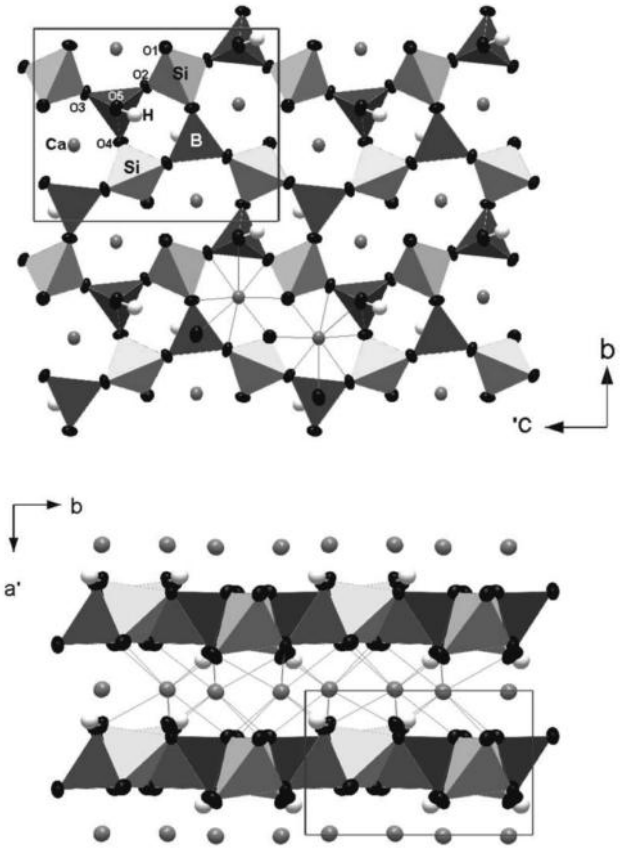

FIGURE 1. Crystal structure of datolite viewed down [100] and [001], based on the structure refinement of the VM datolite at room *T*. Thermal ellipsoid probability: 99%.

nuclear applications. Its use as a neutron absorber (Tarasevich et al. 1991) and in radioactive waste removal (Ojovan and Lee 2005) derives from the observation that borosilicate glasses are suitable for the immobilization of nuclear waste.

Based on the recent study by Zaccarini et al. (2008), the present investigation was undertaken to establish structural details and fundamental thermodynamic parameters of datolite as derived from both room-temperature X-ray diffraction data and the changes induced in the crystal structure and dynamics at low temperatures. Five samples from the study of Zaccarini et al. (2008) and one from the study of Olmi et al. (2000) were investigated. This last sample is from the type locality of Arendal (Norway). The present study was also undertaken as a preliminary work to a neutron diffraction study, which we plan to carry out to exploit the characteristics of datolite as a model sample for this technique (Rinaldi et al. 2009) in terms of both chemical composition (i.e., light elements B and H in the presence of heavy elements, hydrogen bonding) and availability of sufficiently large single crystals.

SAMPLE DESCRIPTION AND MINERALOGY

Datolite commonly occurs in the cavities and veins of basalts and gabbros, and less frequently in granites. It is considered a hydrothermal low-temperature phase (estimated temperature of formation: 430–520 K) and has been used as a petrogenetic indicator of the chemical-physical processes prevailing during hydrothermal crystallization (Zaccarini et al. 2008). The study of Zaccarini et al. (2008) of 10 datolite occurrences in the basalts associated with Mesozoic ophiolites in the Italian Northern Apennines, showed that the fluids responsible for the crystallization of datolite are either modified seawater moving through the oceanic crust by sub-seafloor convective cells, or hydrous solutions circulating throughout the ophiolite sequence under post-oceanic, diagenetic conditions. They suggest that the second alternative is more compatible with the results of trace element and fluid inclusion analysis. Five of the eight localities investigated by Zaccarini et al. (2008) provided a selection of good quality crystals, which were used in the present study. The samples are identified by two letter codes that indicate the datolite localities: BC = Boccassuolo (Modena), CI = Cinghi (Boccassuolo-Modena), CT = Campotrera (Reggio Emilia), SP = Sasso Puzzino (Modena), and VM = Valmozzola (Parma). All samples are from hydrothermal veins in basalts, except SP from an altered gabbro. The CI basalt is rich in sulfides, mainly pyrite. The sample from Arendal (Norway), here named FI (Mineralogical Museum of Florence no. 12468G), was from the same batch as that used in the work by Olmi et al. (2000) and it was selected for its chemical purity (Table 1).

Quantitative electron microprobe analysis in the wavelength dispersive mode (EPMA-WDS) was performed on defect-free polished fragments (part of which provided the crystals used for the X-ray data collection), using a JEOL JXA-8200 electron probe micro-analyzer at the Earth Sciences Department, University of Milan. The system was operated at 10 kV accelerating voltage, 150 nA beam current (measured by a Faraday cup), a 10 µm defocused beam, and counting times of 30 s on the peaks and 10 s on the background. The following natural standards were used: anorthite (Al and Si), tourmaline (B), ilmenite (Ti), grossular (Ca), forsterite (Mg), fayalite (Fe), rhodonite (Mn), barite (Ba), celestite (Sr), omphacite (Na), K-feldspar (K), scapolite (Cl), and F-rich hornblende (F). The data were corrected for matrix effects using the conventional ZAF routine in the JEOL suite of programs. The crystals were homogeneous within analytical error. All datolite samples proved to be exempt of substitutions outside the ideal formula, above the trace level. The chemical

TABLE 1. Average compositions of the 6 datolite samples from different localities (EPMA-WDS analyses)

	VM	BC	CT	SP	CI	FI
SiO_2	36.16	36.39	36.28	35.65	35.59	36.86
B_2O_3	23.68	23.97	23.62	24.09	23.68	23.25
CaO	34.28	33.83	33.77	33.86	33.97	35.00
H_2O*	5.85	5.75	6.29	6.36	6.72	4.86
Total	100.00	100.00	100.00	100.00	100.00	100.00
Formulae based on 10 O atoms						
Si	1.905	1.913	1.901	1.865	1.861	1.964
B	2.152	2.174	2.136	2.175	2.136	2.139
Ca	1.934	1.905	1.896	1.898	1.903	1.999
H	2.055	2.016	2.198	2.219	2.343	1.728
O	10	10	10	10	10	10
Formulae based on 5 O atoms						
Si	0.95	0.96	0.95	0.93	0.93	0.98
Ca	0.97	0.95	0.95	0.95	0.95	1.00
B	1.08	1.09	1.07	1.09	1.07	1.07
H	1.03	1.01	1.10	1.11	1.17	0.86

* H_2O wt% by difference. Ti, Al, Ba, Fe, Sr, Mn, Mg, Na, K, Cl, and F below detection limit.

compositions and formulae, obtained by averaging 10 point analyses per crystal, are provided in Table 1. A slight B excess and Si and Ca deficiency in our EPMA-WDS analysis is ascribed to the difficulty of measuring boron; low-*Z* elements are difficult to analyze quantitatively for several reasons, including low yields and absorption, coupled with high fluorescence of X-rays, non-uniform absorption correction procedures, interference caused by overlaps of higher order X-ray lines, and peak shifts and shape alterations (Bastin and Heijligers 1990; Zaccarini et al. 2008).

X-ray data collection

Diffraction data for six crystals, one from each sample, were collected at T = 298 K using an Oxford Diffraction Gemini diffractometer equipped with an Atlas type detector and with a monochromatic (graphite) beam from a Mo$K\alpha$-radiation source (Enhance X-ray optics) operated at 50 kV and 40 mA. Detector-crystal distance was fixed at 55 mm. A combination of ω and φ scans were used to collect slightly more than a hemisphere of data out to 2θ = 80°, with a fixed exposure time of 5 s per 1° frame (Table 2a). A crystal of datolite from sample VM was used to collect low-T diffraction data. The crystal was slow cooled with a Cryojet open-flow nitrogen gas system (temperature stability better than ±0.1 K and absolute temperature uncertainty at the crystal position less than ±2 K). Intensity data were collected at decreasing temperatures of 280, 250, 220, 190, 160, 130, and 100 K and, on the way back up to room T, at 160, 220, and 280 K. Table 2b provides further details of the data collection techniques.

The diffraction patterns at all T confirm a metrically monoclinic lattice, with reflection conditions consistent with space group $P2_1/c$ (with a ~ 4.83, b ~ 7.61, c ~ 9.63 Å, and β ~ 90.15°). The positions of more than 5000 reflections with a range of d-spacings of 0.55–5.96 Å, corresponding to a θ range of 3.4–40°, were harvested from each data set and used for unit-cell refinements. Although the CI sample shows the largest unit-cell volume and the smallest β-angle among the datolite samples (Table 2a) and has the lowest SiO_2 (35.59 wt%) content and the highest (calculated) amount of H_2O (6.72 wt%) (Table 1), there is no overall trend of cell parameters with composition. We therefore conclude that much of the apparent variation in the unit-cell parameters derives from the influence of peak shapes on the refined peak positions, and from the fact that the formal e.s.d. values given in Table 2 underestimate the true reproducibility. An indication of the true precision is given by the scatter in the cell parameters determined from sample VM at different temperatures, which suggests a true precision of about 1 part in 1000 for cell edges, in agreement with Paciorek et al. (1999). No evidence of non-merohedral twinning was found at any temperature. Lorentz-polarization and analytical absorption corrections by Gaussian integration based upon the physical description of the crystal (CrysAlis, Oxford Diffraction 2009) were performed. The X-ray absorption coefficient is 2.00 mm^{-1} for all samples at all temperatures, assuming an ideal formula of $CaBSiO_4(OH)$.

Structure refinement

The X-ray diffraction data from the crystals of datolite were first processed with the programs E-STATISTICS and ASSIGN-SPACEGROUP, implemented in the WinGX package (Farrugia 1999).

Statistical criteria suggest that datolite is centrosymmetric, and the space group $P2_1/c$ is highly likely. Anisotropic structure refinements were then performed using the SHELX-97 software (Sheldrick 1997), starting from the atomic coordinates of the H-free structure model reported by Foit et al. (1973). Neutral atomic scattering factors for Ca, B, Si, O, and H were taken from

TABLE 2a. Details of data collections and refinements of the six datolite samples at room temperature

Sample	VM	BC	CT	SP	CI	FI
Crystal size (μm³)	35×210×230	60×150×210	80×120×260	35×130×200	50×150×210	50×200×270
a (Å)	4.8354(1)	4.8332(2)	4.8355(1)	4.8336(1)	4.8361(1)	4.8356(1)
b (Å)	7.6082(1)	7.6082(2)	7.6102(1)	7.6076(2)	7.6155(2)	7.6114(1)
c (Å)	9.6335(1)	9.6342(2)	9.6317(1)	9.6298(2)	9.6392(2)	9.6341(2)
β (°)	90.158(1)	90.147(2)	90.150(1)	90.165(2)	90.134(2)	90.158(2)
V (Å³)	354.402(9)	354.267(19)	354.437(9)	354.106(14)	355.004(14)	354.588(11)
Space group	$P2_1/c$	$P2_1/c$	$P2_1/c$	$P2_1/c$	$P2_1/c$	$P2_1/c$
Z	4	4	4	4	4	4
Radiation	Mo$K\alpha$	Mo$K\alpha$	Mo$K\alpha$	Mo$K\alpha$	Mo$K\alpha$	Mo$K\alpha$
Detector type	CCD	CCD	CCD	CCD	CCD	CCD
Crystal-detector distance (mm)	55	55	55	55	55	55
Scan type	ω/ϕ	ω/ϕ	ω/ϕ	ω/ϕ	ω/ϕ	ω/ϕ
Exposure time per frame (s)	5	5	5	5	5	5
θ max (°)	40.08	40.12	40.08	40.07	40.10	40.08
	$-8 \le h \le 8$	$-8 \le h \le 8$	$-8 \le h \le 7$	$-7 \le h \le 8$	$-8 \le h \le 8$	$-8 \le h \le 8$
	$-12 \le k \le 13$	$-13 \le k \le 13$	$-13 \le k \le 13$	$-13 \le k \le 13$	$-13 \le k \le 13$	$-13 \le k \le 13$
	$-17 \le l \le 17$	$-16 \le l \le 17$	$-16 \le l \le 17$	$-17 \le l \le 15$	$-17 \le l \le 16$	$-17 \le l \le 17$
No. measured reflections	8499	7933	7893	7902	7971	8202
No. unique reflections	2201	2192	2211	2188	2212	2206
No. unique reflections with $F_o > 4\sigma(F_o)$	1932	1984	2081	1924	2005	2006
No. refined parameters	78	78	78	78	77	78
R_{int}	0.0321	0.0668	0.0578	0.1225	0.0498	0.0358
R_1 (F) with $F_o > 4\sigma(F_o)$	0.0218	0.0375	0.0346	0.0528	0.0322	0.0228
wR_2 (F^2)	0.0447	0.0835	0.0885	0.1190	0.0778	0.0557
GooF	1.446	1.813	1.805	1.522	1.613	1.429
Weighting scheme: a, b	0.01,0	0.02,0	0.03,0	0.03,0	0.025,0	0.02,0
Residuals (e^-/Å³)	+0.6/–0.4	+0.8/–1.1	+0.7/–0.9	–1.1/+1.1	+0.8/–0.6	+0.7/–0.5

Note: $R_{int} = \Sigma|F^2_{obs} - F^2_{obs}(mean)|/\Sigma[F^2_{obs}]$; $R_1 = \Sigma(||F_{obs}| - |F_{calc}||)/\Sigma|F_{obs}|$; $wR_2 = \{\Sigma[w(F^2_{obs} - F^2_{calc})^2]/\Sigma[w(F^2_{obs})^2]\}^{0.5}$, $w = 1/[\sigma^2(F^2_{obs}) + (a^*P)^2 + b^*P]$, $P = [Max(F^2_{obs},0) + 2^*F^2_{calc}]/3$.

TABLE 2b. Details of data collections and refinements of "VM" datolite at different temperatures

T (K)	280	250	220	190	160	130	100	160*	220*	280*
Crystal size (μm³)	35×210×230	35×210×230	35×210×230	35×210×230	35×210×230	35×210×230	35×210×230	35×210×230	35×210×230	35×210×230
a (Å)	4.8355(1)	4.8330(1)	4.8325(1)	4.8308(1)	4.8303(1)	4.8298(1)	4.8284(1)	4.8311(1)	4.8328(1)	4.83630(10)
b (Å)	7.6085(1)	7.6074(1)	7.6041(1)	7.6011(1)	7.6011(1)	7.6002(1)	7.5995(1)	7.6000(1)	7.6078(1)	7.61000(10)
c (Å)	9.6326(2)	9.6310(2)	9.6300(2)	9.6290(2)	9.6292(2)	9.6321(2)	9.6310(2)	9.6311(2)	9.6313(1)	9.6348(2)
β (°)	90.159(2)	90.175(2)	90.184(2)	90.176(2)	90.180(2)	90.183(2)	90.180(2)	90.169(2)	90.173(2)	90.158(2)
V (Å³)	354.391(11)	354.097(11)	353.870(11)	353.569(11)	353.540(11)	353.568(11)	353.393(11)	353.617(11)	354.112(9)	354.600(11)
Space group	$P2_1/c$	$P2_1/c$	$P2_1/c$	$P2_1/c$	$P2_1/c$	$P2_1/c$	$P2_1/c$	$P2_1/c$	$P2_1/c$	$P2_1/c$
Z	4	4	4	4	4	4	4	4	4	4
Radiation	MoKα	MoKα	MoKα	MoKα	MoKα	MoKα	MoKα	MoKα	MoKα	MoKα
Detector type	CCD	CCD	CCD	CCD	CCD	CCD	CCD	CCD	CCD	CCD
Crystal-detector distance (mm)	55	55	55	55	55	55	55	55	55	55
Scan type	ω/φ	ω/φ	ω/φ	ω/φ	ω/φ	ω/φ	ω/φ	ω/φ	ω/φ	ω/φ
Exposure time per frame (s)	5	5	5	5	5	5	5	5	5	5
θ max (°)	40.09	40.07	40.08	40.10	40.10	40.11	40.11	40.10	40.07	40.10
	$-7 \le h \le 8$	$-7 \le h \le 8$	$-7 \le h \le 8$	$-7 \le h \le 8$	$-7 \le h \le 8$	$-7 \le h \le 8$	$-7 \le h \le 8$	$-7 \le h \le 8$	$-7 \le h \le 8$	$-7 \le h \le 8$
	$-13 \le k \le 13$	$-13 \le k \le 13$	$-13 \le k \le 13$	$-13 \le k \le 13$	$-13 \le k \le 13$	$-13 \le k \le 13$	$-13 \le k \le 13$	$-13 \le k \le 13$	$-13 \le k \le 13$	$-13 \le k \le 13$
	$-16 \le l \le 17$	$-16 \le l \le 17$	$-16 \le l \le 17$	$-16 \le l \le 17$	$-16 \le l \le 17$	$-16 \le l \le 17$	$-16 \le l \le 17$	$-16 \le l \le 17$	$-16 \le l \le 17$	$-16 \le l \le 17$
No. measured reflections	8553	8569	8509	8520	8540	8549	8543	8537	8566	8591
No. unique reflections	2205	2204	2204	2200	2203	2200	2197	2203	2204	2207
No. unique reflections with $F_o > 4\sigma(F_o)$	1921	1933	1934	1942	1933	1942	1940	1930	1921	1930
No. refined parameters	83	78	78	78	77	78	78	78	78	78
R_{int}	0.0329	0.0331	0.0334	0.0315	0.0313	0.0317	0.0323	0.0334	0.0332	0.0348
R_1 (F) with $F_o > 4\sigma(F_o)$	0.0223	0.0223	0.0216	0.0212	0.0208	0.0203	0.0195	0.0211	0.0213	0.0226
wR_2 (F^2)	0.0481	0.0476	0.0471	0.0444	0.0442	0.0433	0.0420	0.0467	0.0472	0.0506
GooF	1.542	1.517	1.497	1.457	1.460	1.428	1.387	1.502	1.526	1.370
Weighting scheme: *a, b*	0.01,0	0.01,0	0.01,0	0.01,0	0.01,0	0.01,0	0.01,0	0.01,0	0.01,0	0.01,0
Residuals (e^-/Å³)	+0.6/–0.4	+0.6/–0.4	+0.6/–0.4	+0.5/–0.3	+0.5/–0.4	+0.5/–0.4	+0.6/–0.4	+0.6/–0.5	+0.5/–0.4	+0.6/–0.4

Note: $R_{int} = \Sigma|F^2_{obs} - F^2_{obs}(\text{mean})|/\Sigma[F^2_{obs}]$; $R_1 = \Sigma(||F_{obs}| - |F_{calc}||)/\Sigma|F_{obs}|$; $wR_2 = \{\Sigma[w(F^2_{obs} - F^2_{calc})^2]/\Sigma[w(F^2_{obs})^2]\}^{0.5}$, $w = 1/[\sigma^2(F^2_{obs}) + (a*P)^2 + b*P]$, $P = [\text{Max}(F^2_{obs}, 0) + 2*F^2_{calc}]/3$.
* Data collected increasing *T*.

the *International Tables for Crystallography* (Wilson and Prince 1999). The secondary isotropic extinction effect was corrected according to Larson's formalism (1967), as implemented in the SHELXL-97 package. The refinement was conducted assuming a fully ordered distribution of Si and B in the tetrahedral sites. The H-site was identified on the basis of the maxima in the difference-Fourier maps of the electron density and was refined isotropically (Tables 3a and 3b). No restraints on bond distances or angles were used. Convergence was rapidly achieved after a few least-square cycles of refinement and the variance-covariance matrix did not show any significant correlation between the refined parameters. At the end of the refinements, the residual electron density in the difference-Fourier maps was almost insignificant (Tables 2a and 2b). Refined site positions and thermal displacement parameters are listed in Tables 3a and 3b. Bond distances and angles of the datolite sample VM at decreasing temperatures (i.e., 280, 250, 220, 190, 160, 130, and 100 K) are given in Table 4. Bond distances and angles obtained on heating back to room *T* in three steps (i.e., 160, 220, and 280 K) and those of the other datolite samples at room conditions (i.e., FI, BC, CT, SP, and CI) are deposited[1] (as CIF). There is almost no significant variation in bond lengths between samples at room *T*. The largest differences are represented by slightly longer Ca-O bond distances in CI datolite than in the other samples. For example, Ca-O3′ is 2.6616(8) Å and Ca-O5′ is 2.6742(8) Å in CI, whereas Ca-O3′ is 2.6583(6) Å and Ca-O5′ is 2.6705(6) Å in VM (Tables 4 and 5[1]). However, the Si- and B-tetrahedra in CI show bond distances and angles that are identical within uncertainties to those in the other datolite crystals.

RESULTS: LOW-*T* ELASTIC BEHAVIOR AND STRUCTURE DYNAMICS

The variation of the unit-cell parameters of the VM datolite crystal as a function of *T* is shown in Figure 2. Each trend is continuous, with no thermoelastic anomaly or phase transition within the *T*-range investigated. The expansion of datolite seems to be dominated by the axial expansion along [100] and [010], whereas the *c*-axis length is almost unaffected by the *T*-variation (Fig. 2). A weighted polynomial regression through *a* vs. *T* and *b* vs. *T* data points yields: $a_T = a_{100K} - 4(4)\cdot10^{-5}T + 1.0(1)\cdot10^{-7}T^2$ ($R^2 = 0.95$) and $b_T = b_{100K} - 4.8(5)\cdot10^{-5}T + 2.6(1)\cdot10^{-7}\ T^2$ ($R^2 = 0.95$). The β unit-cell angle shows a slight increase at low temperature. The volume thermal expansion coefficient ($\alpha_V = V^{-1}\ \partial V/\partial T$) between 100 and 280 K, calculated by weighted linear regression, is $\alpha_V = 1.5(2)\cdot10^{-5}K^{-1}$.

The higher thermal expansion of datolite along the *a*-axis is due to the layered nature of its structure; the Ca-O bond distances are the most compressible and expandable, and govern the contraction along a direction perpendicular to the polyhedral layers (Fig. 1) parallel to (100). The "tetrahedral layer" is significantly more rigid. The 8-membered rings lying on (100) are actually comprised of four adjacent "building block units" of 4-membered rings, which behave as rigid-units, although they are allowed

[1] Deposit item AM-10-044, CIFs and Table 5. Deposit items are available two ways: For a paper copy contact the Business Office of the Mineralogical Society of America (see inside front cover of recent issue) for price information. For an electronic copy visit the MSA web site at http://www.minsocam.org, go to the *American Mineralogist* Contents, find the table of contents for the specific volume/issue wanted, and then click on the deposit link there.

TABLE 3a. Refined position and thermal displacement parameters (Å^2) of datolites at room temperature

	x	*y*	*z*	U_{11}	U_{22}	U_{33}	U_{23}	U_{13}	U_{12}	U_{eq}/U_{iso}
					VM					
Ca	0.00832(3)	0.60617(2)	0.16388(2)	0.0068(1)	0.0071(1)	0.0055(1)	0.0000(1)	0.0004(1)	0.0005(1)	0.0064(1)
Si	0.46883(4)	0.26615(3)	0.08438(2)	0.0052(1)	0.0042(1)	0.0034(1)	−0.0002(1)	0.0000(1)	0.0003(1)	0.0043(1)
B	0.56839(18)	0.08950(11)	−0.15909(9)	0.0053(3)	0.0059(3)	0.0042(3)	0.0003(2)	0.0007(2)	0.0002(3)	0.0051(2)
O1	0.24051(13)	0.40104(8)	0.03745(6)	0.0083(2)	0.0071(2)	0.0068(3)	−0.0001(2)	−0.0008(2)	0.0024(2)	0.0074(1)
O2	0.66987(12)	0.19903(7)	−0.04273(6)	0.0071(2)	0.0070(2)	0.0049(2)	−0.0019(2)	0.0009(2)	−0.0010(2)	0.0063(1)
O3	0.67508(12)	0.33472(8)	0.21044(6)	0.0064(2)	0.0084(2)	0.0039(2)	−0.0016(2)	0.0003(2)	0.0003(2)	0.0062(1)
O4	0.31509(12)	0.08787(7)	0.14600(6)	0.0080(2)	0.0043(2)	0.0086(3)	0.0008(2)	0.0024(2)	0.0003(2)	0.0070(1)
O5	0.25854(13)	0.08652(8)	−0.16342(7)	0.0055(2)	0.0103(2)	0.0063(3)	0.0009(2)	0.0004(2)	−0.0007(2)	0.0074(1)
H	0.207(3)	0.0523(18)	−0.0879(17)							0.029(4)
					BC					
Ca	0.00835(4)	0.60619(3)	0.16389(2)	0.0073(1)	0.0079(1)	0.0049(1)	0.0001(1)	−0.0002(1)	0.0005(1)	0.0067(1)
Si	0.46894(6)	0.26609(4)	0.08439(3)	0.0057(1)	0.0050(1)	0.0027(1)	−0.0003(1)	−0.0007(1)	0.0006(1)	0.0045(1)
B	0.5685(3)	0.08941(15)	−0.15925(12)	0.0067(4)	0.0065(4)	0.0035(4)	0.0003(3)	−0.0003(3)	0.0006(3)	0.0056(2)
O1	0.24029(18)	0.40110(11)	0.03750(9)	0.0083(3)	0.0087(3)	0.0066(3)	−0.0004(2)	−0.0020(3)	0.0029(2)	0.0079(2)
O2	0.67035(17)	0.19913(11)	−0.04276(8)	0.0075(3)	0.0086(3)	0.0040(3)	−0.0019(2)	0.0007(2)	−0.0012(2)	0.0067(2)
O3	0.67535(17)	0.33466(11)	0.21047(8)	0.0073(3)	0.0096(3)	0.0029(3)	−0.0017(2)	−0.0007(2)	0.0000(2)	0.0066(2)
O4	0.31490(18)	0.08794(11)	0.14605(9)	0.0082(3)	0.0055(3)	0.0080(3)	0.0008(2)	0.0016(2)	0.0004(2)	0.0072(2)
O5	0.25877(18)	0.08655(12)	−0.16350(9)	0.0063(3)	0.0106(3)	0.0062(3)	0.0008(3)	−0.0003(2)	−0.0011(2)	0.0077(2)
H	0.216(5)	0.037(3)	−0.096(3)							0.028(6)
					CT					
Ca	0.00835(4)	0.60622(2)	0.16387(2)	0.0058(1)	0.0073(1)	0.0058(1)	0.0000(1)	0.0002(1)	0.0005(1)	0.0063(1)
Si	0.46903(5)	0.26609(3)	0.08442(3)	0.0043(1)	0.0046(1)	0.0039(1)	−0.0002(1)	−0.0002(1)	0.0003(1)	0.0042(1)
B	0.5682(2)	0.08946(13)	−0.15914(11)	0.0048(3)	0.0058(3)	0.0048(4)	−0.0002(3)	0.0001(3)	−0.0002(3)	0.0051(2)
O1	0.24040(16)	0.40095(9)	0.03741(8)	0.0077(3)	0.0076(3)	0.0077(3)	−0.0002(2)	−0.0014(2)	0.0025(2)	0.0077(2)
O2	0.66992(14)	0.19887(9)	−0.04268(8)	0.0059(2)	0.0077(3)	0.0051(3)	−0.0023(2)	0.0011(2)	−0.0012(2)	0.0062(2)
O3	0.67513(14)	0.33452(10)	0.21048(7)	0.0055(2)	0.0085(3)	0.0043(3)	−0.0018(2)	−0.0003(2)	0.0000(2)	0.0061(2)
O4	0.31507(15)	0.08816(9)	0.14600(8)	0.0070(3)	0.0046(2)	0.0094(3)	0.0007(2)	0.0025(2)	0.0005(2)	0.0070(2)
O5	0.25878(15)	0.08650(10)	−0.16356(8)	0.0045(3)	0.0107(3)	0.0066(3)	0.0011(2)	0.0003(2)	−0.0006(2)	0.0073(2)
H	0.199(4)	0.048(3)	−0.088(3)							0.022(6)
					SP					
Ca	0.00828(5)	0.60620(4)	0.16386(3)	0.0058(1)	0.0066(1)	0.0062(1)	−0.0001(1)	0.0000(1)	0.0005(1)	0.0062(1)
Si	0.46889(8)	0.26612(5)	0.08436(4)	0.0040(2)	0.0040(2)	0.0042(2)	−0.0004(1)	−0.0004(1)	0.0005(1)	0.0041(1)
B	0.5686(3)	0.0894(2)	−0.15918(16)	0.0047(5)	0.0056(5)	0.0057(6)	0.0002(4)	−0.0004(4)	0.0002(4)	0.0053(3)
O1	0.2400(2)	0.40078(14)	0.03753(12)	0.0069(4)	0.0070(4)	0.0075(4)	0.0001(3)	−0.0013(3)	0.0031(3)	0.0071(2)
O2	0.6697(2)	0.19901(14)	−0.04245(11)	0.0056(4)	0.0071(4)	0.0054(4)	−0.0022(3)	0.0004(3)	−0.0010(3)	0.0060(2)
O3	0.6754(2)	0.33464(15)	0.21044(11)	0.0054(4)	0.0079(4)	0.0047(4)	−0.0022(3)	−0.0005(3)	0.0002(3)	0.0060(2)
O4	0.3153(2)	0.08795(14)	0.14589(12)	0.0069(4)	0.0039(4)	0.0104(5)	0.0010(3)	0.0021(3)	−0.0002(3)	0.0071(3)
O5	0.2586(2)	0.08613(15)	−0.16341(12)	0.0047(4)	0.0097(4)	0.0074(4)	0.0006(3)	0.0002(3)	−0.0010(3)	0.0073(2)
H	0.205(7)	0.051(4)	−0.094(5)							0.037(10)
					CI					
Ca	0.00838(4)	0.60613(2)	0.16386(2)	0.0073(1)	0.0071(1)	0.0066(1)	0.0000(1)	0.0004(1)	0.0004(1)	0.0070(1)
Si	0.46897(5)	0.26613(3)	0.08442(3)	0.0057(1)	0.0044(1)	0.0045(1)	−0.0002(1)	0.0000(1)	0.0003(1)	0.0048(1)
B	0.5685(2)	0.08943(13)	−0.15906(11)	0.0067(4)	0.0061(4)	0.0049(3)	0.0004(3)	0.0004(3)	0.0000(3)	0.0059(2)
O1	0.24048(16)	0.40086(9)	0.03762(8)	0.0090(3)	0.0075(3)	0.0079(3)	−0.0003(2)	−0.0011(2)	0.0025(2)	0.0081(2)
O2	0.67002(15)	0.19910(9)	−0.04259(7)	0.0074(3)	0.0077(3)	0.0058(2)	−0.0021(2)	0.0012(2)	−0.0013(2)	0.0070(2)
O3	0.67496(15)	0.33448(10)	0.21036(7)	0.0073(3)	0.0084(3)	0.0051(2)	−0.0015(2)	−0.0004(2)	0.0001(2)	0.0069(2)
O4	0.31472(16)	0.08787(9)	0.14591(8)	0.0083(3)	0.0049(3)	0.0100(3)	0.0010(2)	0.0024(2)	0.0001(2)	0.0077(2)
O5	0.25896(15)	0.08649(10)	−0.16333(8)	0.0061(3)	0.0102(3)	0.0075(3)	0.0009(2)	0.0008(2)	−0.0006(2)	0.0079(2)
H	0.214(5)	0.048(3)	−0.094(3)							0.032(6)
					FI					
Ca	0.00832(3)	0.60617(2)	0.16393(1)	0.0064(1)	0.0073(1)	0.0056(1)	0.0000(1)	0.0003(1)	0.0005(1)	0.0064(1)
Si	0.46891(4)	0.26615(3)	0.08439(2)	0.0050(1)	0.0047(1)	0.0034(1)	−0.0003(1)	−0.0002(1)	0.0004(1)	0.0044(1)
B	0.56794(17)	0.08929(11)	−0.15911(8)	0.0055(3)	0.0056(3)	0.0042(3)	0.0004(2)	0.0003(2)	−0.0002(2)	0.0051(2)
O1	0.24076(12)	0.40091(7)	0.03742(6)	0.0084(2)	0.0080(2)	0.0069(2)	−0.0003(2)	−0.0010(2)	0.0026(2)	0.0078(1)
O2	0.67004(11)	0.19900(7)	−0.04251(5)	0.0066(2)	0.0073(2)	0.0050(2)	−0.0019(2)	0.0007(2)	−0.0015(2)	0.0063(1)
O3	0.67495(11)	0.33449(8)	0.21045(5)	0.0062(2)	0.0083(2)	0.0039(2)	−0.0017(2)	−0.0001(2)	−0.0001(2)	0.0062(1)
O4	0.31495(12)	0.08789(7)	0.14598(6)	0.0075(2)	0.0053(2)	0.0084(2)	0.0007(2)	0.0023(2)	0.0004(2)	0.0071(1)
O5	0.25883(12)	0.08650(8)	−0.16350(6)	0.0054(2)	0.0104(2)	0.0065(2)	0.0008(2)	0.0002(2)	−0.0007(2)	0.0074(1)
H	0.213(4)	0.047(2)	−0.0930(18)							0.030(4)

Notes: The anisotropic displacement factor exponent takes the form: $-2\pi^2[(ha^*)^2U_{11}+\ldots+2hka^*b^*U_{12}]$. U_{eq} is defined as one third of the trace of the orthogonalized U_{ij} tensor.

by symmetry to shear and tilt as do the 4-membered rings in feldspars (cf. Megaw 1974). There is no evidence in datolite for such changes at low temperature.

Intra-polyhedral bond distances and angles show common features in all samples at room *T*: (1) the Si-tetrahedron is strongly deformed, with Si-O distances ranging between ~1.57 and ~1.66 Å and O-Si-O angles ranging between ~105.4 and ~115.3° (Tables 4 and 5[1]); (2) the B-tetrahedron is almost regular (Tables 4 and 5[1]); (3) the Ca-polyhedron is significantly distorted, with bond distances ranging between ~2.28 and ~2.67 Å (considering a coordination number CN = 8) (Tables 4 and 5[1]); and (4) only one independent H-site occurs and its refined position suggests a bifurcated hydrogen bonding scheme with O5 as donor and O4 and O2 as acceptors (with O5-H ~ 0.8 Å) and: (1) O5···O4 ~ 2.99 Å, H···O4 ~ 2.33 Å, and O5-H···O4 ~ 140°, and (2) O5···O2 ~ 2.96 Å, H···O2 ~ 2.36 Å, and O5-H···O2

TABLE 3b. Refined position and thermal displacement parameters (Å^2) of VM datolite at different temperatures

	x	*y*	*z*	U_{11}	U_{22}	U_{33}	U_{23}	U_{13}	U_{12}	U_{eq}/U_{iso}
					280 K					
Ca	0.00833(4)	0.60616(2)	0.16388(2)	0.0065(1)	0.0068(1)	0.0053(1)	0.0000(1)	0.0006(1)	0.0004(1)	0.0062(1)
Si	0.46899(5)	0.26620(3)	0.08436(2)	0.0049(1)	0.0043(1)	0.0031(1)	–0.0002(1)	0.0002(1)	0.0003(1)	0.0041(1)
B	0.56856(19)	0.08933(12)	–0.15914(10)	0.0059(3)	0.0056(3)	0.0040(3)	0.0003(3)	0.0001(3)	0.0002(3)	0.0052(2)
O1	0.24063(13)	0.40112(8)	0.03738(7)	0.0076(3)	0.0073(2)	0.0068(3)	–0.0003(2)	–0.0010(2)	0.0022(2)	0.0072(2)
O2	0.66991(12)	0.19903(8)	–0.04253(7)	0.0066(2)	0.0071(2)	0.0045(2)	-0.0018(2)	0.0010(2)	–0.0008(2)	0.0061(1)
O3	0.67520(12)	0.33451(8)	0.21047(6)	0.0061(3)	0.0083(2)	0.0038(2)	–0.0015(2)	0.0004(2)	0.0004(2)	0.0061(1)
O4	0.31489(13)	0.08791(8)	0.14591(7)	0.0074(3)	0.0046(2)	0.0082(3)	0.0009(2)	0.0024(2)	0.0004(2)	0.0067(2)
O5	0.25889(14)	0.08651(9)	–0.16344(7)	0.0054(3)	0.0099(3)	0.0061(3)	0.0011(2)	0.0006(2)	–0.0008(2)	0.0071(2)
H	0.206(3)	0.048(2)	–0.092(2)	0.012(9)	0.032(11)	0.046(15)	–0.003(10)	–0.005(9)	0.006(8)	0.030(7)
					250 K					
Ca	0.00835(3)	0.60620(2)	0.16389(2)	0.0060(1)	0.0061(1)	0.0047(1)	0.0001(1)	0.0005(1)	0.0004(1)	0.0056(1)
Si	0.46911(5)	0.26634(3)	0.08435(2)	0.0047(1)	0.0038(1)	0.0029(1)	–0.0001(1)	0.0002(1)	0.0003(1)	0.0038(1)
B	0.56831(19)	0.08931(11)	–0.15912(10)	0.0053(3)	0.0053(3)	0.0036(3)	0.0001(3)	0.0004(3)	0.0004(3)	0.0047(2)
O1	0.24073(13)	0.40130(8)	0.03729(7)	0.0070(3)	0.0066(2)	0.0060(3)	–0.0003(2)	–0.0006(2)	0.0019(2)	0.0065(2)
O2	0.67008(12)	0.19905(8)	–0.04246(6)	0.0064(2)	0.0066(2)	0.0043(2)	–0.0017(2)	0.0007(2)	–0.0010(2)	0.0058(1)
O3	0.67541(12)	0.33463(8)	0.21049(6)	0.0059(2)	0.0076(2)	0.0032(2)	–0.0013(2)	0.0007(2)	0.0003(2)	0.0056(1)
O4	0.31504(13)	0.08798(7)	0.14594(7)	0.0071(3)	0.0045(2)	0.0070(3)	0.0008(2)	0.0025(2)	0.0002(2)	0.0062(2)
O5	0.25889(13)	0.08654(8)	–0.16348(7)	0.0048(2)	0.0091(3)	0.0055(3)	0.0010(2)	0.0006(2)	–0.0010(2)	0.0065(2)
H	0.207(4)	0.050(2)	–0.092(2)							0.035(5)
					220 K					
Ca	0.00828(3)	0.60625(2)	0.16393(2)	0.0052(1)	0.0055(1)	0.0043(1)	0.0000(1)	0.0006(1)	0.0004(1)	0.0050(1)
Si	0.46932(5)	0.08433(2)	0.26637(3)	0.0042(1)	0.0036(1)	0.0025(1)	–0.0002(1)	0.0003(1)	0.0003(1)	0.0035(1)
B	0.56882(19)	0.08946(11)	–0.15909(9)	0.0049(3)	0.0050(3)	0.0034(3)	0.0003(3)	0.0006(3)	0.0001(3)	0.0044(2)
O1	0.24116(13)	0.40145(8)	0.03713(7)	0.0063(2)	0.0063(2)	0.0055(2)	–0.0002(2)	–0.0003(2)	0.0017(2)	0.0060(1)
O2	0.67052(12)	0.19898(8)	–0.04243(6)	0.0057(2)	0.0062(2)	0.0039(2)	–0.0010(2)	0.0008(2)	–0.0008(2)	0.0053(1)
O3	0.67577(12)	0.33471(8)	0.21049(6)	0.0051(2)	0.0068(2)	0.0031(2)	–0.0011(2)	0.0004(2)	0.0004(2)	0.0050(1)
O4	0.31490(12)	0.08820(7)	0.14588(7)	0.0061(2)	0.0041(2)	0.0069(3)	0.0008(2)	0.0022(2)	0.0002(2)	0.0057(1)
O5	0.25916(13)	0.08658(8)	–0.16354(7)	0.0046(2)	0.0083(2)	0.0049(3)	0.0012(2)	0.0005(2)	–0.0007(2)	0.0059(1)
H	0.207(3)	0.0492(19)	–0.0973(19)							0.025(4)
					190 K					
Ca	0.00821(3)	0.60626(2)	0.16395(2)	0.0047(1)	0.0049(1)	0.0039(1)	0.0001(1)	0.0003(1)	0.0003(1)	0.0045(1)
Si	0.46940(4)	0.26645(3)	0.08429(2)	0.0038(1)	0.0032(1)	0.0023(1)	–0.0002(1)	0.0001(1)	0.0002(1)	0.0031(1)
B	0.56919(18)	0.08924(11)	–0.15927(9)	0.0044(3)	0.0042(3)	0.0037(3)	–0.0001(2)	0.0001(3)	0.0001(2)	0.0041(2)
O1	0.24095(12)	0.40161(7)	0.03728(6)	0.0059(2)	0.0053(2)	0.0049(2)	–0.0003(2)	–0.0004(2)	0.0016(2)	0.0054(1)
O2	0.67107(12)	0.19886(7)	–0.04244(6)	0.0053(2)	0.0055(2)	0.0035(2)	–0.0015(2)	0.0006(2)	–0.0005(2)	0.0048(1)
O3	0.67594(12)	0.33462(7)	0.21057(6)	0.0051(2)	0.0060(2)	0.0028(2)	–0.0011(2)	0.0001(2)	0.0000(2)	0.0046(1)
O4	0.31449(12)	0.08821(7)	0.14588(6)	0.0058(2)	0.0037(2)	0.0059(2)	0.0006(2)	0.0018(2)	0.0001(2)	0.0051(1)
O5	0.25875(12)	0.08665(8)	–0.16356(7)	0.0041(2)	0.0076(2)	0.0047(2)	0.0009(2)	0.0003(2)	–0.0006(2)	0.0055(1)
H	0.203(3)	0.0537(18)	–0.0901(17)							0.024(4)
					160 K					
Ca	0.00823(3)	0.60628(2)	0.16398(2)	0.0043(1)	0.0044(1)	0.0036(1)	0.0000(1)	0.0004(1)	0.0002(1)	0.0041(1)
Si	0.46953(4)	0.26652(3)	0.08426(2)	0.0035(1)	0.0032(1)	0.0024(1)	–0.0001(1)	0.0002(1)	0.0002(1)	0.0030(1)
B	0.56915(18)	0.08918(11)	–0.15908(9)	0.0041(3)	0.0041(3)	0.0035(3)	0.0002(2)	0.0003(3)	–0.0002(2)	0.0039(2)
O1	0.24119(12)	0.40174(7)	0.03721(6)	0.0053(2)	0.0052(2)	0.0046(2)	–0.0004(2)	0.0000(2)	0.0012(2)	0.0050(1)
O2	0.67100(11)	0.19902(7)	–0.04245(6)	0.0048(2)	0.0051(2)	0.0036(2)	–0.0011(2)	0.0004(2)	–0.0005(2)	0.0045(1)
O3	0.67631(11)	0.33466(7)	0.21064(6)	0.0046(2)	0.0056(2)	0.0029(2)	–0.0011(2)	0.0002(2)	0.0001(2)	0.0044(1)
O4	0.31466(12)	0.08819(7)	0.14591(6)	0.0052(2)	0.0031(2)	0.0059(2)	0.0006(2)	0.0016(2)	0.0001(2)	0.0047(1)
O5	0.25889(12)	0.08670(8)	–0.16354(6)	0.0036(2)	0.0069(2)	0.0044(2)	0.0009(2)	0.0001(2)	–0.0006(2)	0.0050(1)
H	0.212(3)	0.0522(19)	–0.0868(18)							0.032(4)
					130 K					
Ca	0.00821(3)	0.60628(2)	0.16398(2)	0.0037(1)	0.0039(1)	0.0030(1)	0.0001(1)	0.0003(1)	0.0002(1)	0.0035(1)
Si	0.46966(4)	0.26660(3)	0.08426(2)	0.0030(1)	0.0027(1)	0.0021(1)	–0.0001(1)	0.0002(1)	0.0001(1)	0.0026(1)
B	0.56930(17)	0.08934(10)	–0.15908(9)	0.0036(3)	0.0041(3)	0.0029(3)	0.0000(2)	0.0002(2)	–0.0001(2)	0.0035(2)
O1	0.24102(12)	0.40192(7)	0.03711(6)	0.0045(2)	0.0042(2)	0.0043(2)	–0.0002(2)	–0.0004(2)	0.0011(2)	0.0043(1)
O2	0.67129(11)	0.19890(7)	–0.04238(6)	0.0043(2)	0.0045(2)	0.0032(2)	–0.0009(2)	0.0005(2)	–0.0002(2)	0.0040(1)
O3	0.67642(11)	0.33458(7)	0.21062(6)	0.0042(2)	0.0048(2)	0.0025(2)	–0.0009(2)	0.0003(2)	0.0001(2)	0.0038(1)
O4	0.31455(11)	0.08837(7)	0.14577(6)	0.0046(2)	0.0031(2)	0.0048(2)	0.0004(2)	0.0013(2)	0.0001(2)	0.0042(1)
O5	0.25886(12)	0.08678(7)	–0.16344(6)	0.0033(2)	0.0063(2)	0.0041(2)	0.0009(2)	0.0007(2)	–0.0005(2)	0.0046(1)
H	0.203(3)	0.0514(18)	–0.0883(17)							0.025(4)
					100 K					
Ca	0.00814(3)	0.60632(2)	0.16403(2)	0.0033(1)	0.0035(1)	0.0026(1)	0.0000(1)	0.0002(1)	0.0002(1)	0.0031(1)
Si	0.46979(4)	0.26666(3)	0.08422(2)	0.0028(1)	0.0025(1)	0.0018(1)	–0.0001(1)	0.0002(1)	0.0002(1)	0.0024(1)
B	0.56934(17)	0.08914(10)	–0.15888(9)	0.0036(3)	0.0033(3)	0.0030(3)	0.0001(2)	–0.0001(2)	–0.0001(2)	0.0033(2)
O1	0.24114(11)	0.40207(7)	0.03707(6)	0.0041(2)	0.0044(2)	0.0039(2)	–0.0001(2)	–0.0004(2)	0.0008(2)	0.0041(1)
O2	0.67150(11)	0.19890(7)	–0.04237(6)	0.0041(2)	0.0041(2)	0.0028(2)	–0.0009(2)	0.0006(2)	–0.0004(2)	0.0037(1)
O3	0.67669(11)	0.33469(7)	0.21060(6)	0.0037(2)	0.0047(2)	0.0022(2)	–0.0008(2)	0.0004(2)	0.0001(2)	0.0035(1)
O4	0.31451(11)	0.08842(7)	0.14588(6)	0.0042(2)	0.0029(2)	0.0045(2)	0.0004(2)	0.0010(2)	0.0002(2)	0.0039(1)
O5	0.25872(11)	0.08669(7)	–0.16351(6)	0.0032(2)	0.0057(2)	0.0036(2)	0.0008(2)	0.0004(2)	–0.0006(2)	0.0042(1)
H	0.208(3)	0.0511(19)	–0.0874(18)							0.029(4)

Notes: The anisotropic displacement factor exponent takes the form: $-2\pi^2[(ha^*)^2U_{11} + \ldots + 2hka^*b^*U_{12}]$. U_{eq} is defined as one third of the trace of the orthogonalized U_{ij} tensor. At 280 K, the H-site was successfully refined anisotropically.

TABLE 4. Bond distances (Å) and angles (°) in the structure of VM datolite at different temperatures

T (K)	300	280	250	220	190	160	130	100
Si-O1	1.5728(7)	1.5733(7)	1.5731(7)	1.5729(7)	1.5733(6)	1.5732(6)	1.5749(6)	1.5751(6)
Si-O2	1.6468(6)	1.6449(7)	1.6445(6)	1.6449(6)	1.6460(6)	1.6451(6)	1.6458(6)	1.6455(6)
Si-O3	1.6537(6)	1.6533(6)	1.6530(6)	1.6534(6)	1.6538(6)	1.6551(6)	1.6546(6)	1.6550(6)
Si-O4	1.6575(6)	1.6581(7)	1.6583(6)	1.6573(6)	1.6583(6	1.6590(6)	1.6583(6)	1.6590(6)
<Si-O>	1.6327	1.6324	1.6322	1.6321	1.6328	1.6331	1.6334	1.6336
B-O2	1.4794(10)	1.4817(11)	1.4825(11)	1.4811(10)	1.4828(10)	1.4822(10)	1.4819(10)	1.4815(10)
B-O3	1.4771(10)	1.4774(11)	1.4777(11)	1.4769(10)	1.4750(10)	1.4768(10)	1.4769(10)	1.4792(10)
B-O4	1.4677(10)	1.4670(11)	1.4672(10)	1.4685(10)	1.4667(10)	1.4657(10)	1.4680(9)	1.4665(9)
B-O5	1.4989(11)	1.4980(11)	1.4960(11)	1.4971(11)	1.5002(10)	1.4993(10)	1.4999(10)	1.5004(10)
<B-O>	1.4808	1.4810	1.4808	1.4809	1.4812	1.4810	1.4817	1.4819
Ca-O1	2.2776(6)	2.2777(7)	2.2773(6)	2.2782(6)	2.2760(6)	2.2764(6)	2.2757(6)	2.2757(6)
Ca-O1′	2.2802(6)	2.2799(7)	2.2786(6)	2.2785(6)	2.2788(6)	2.2790(6)	2.2781(6)	2.2780(6)
Ca-O4	2.4156(6)	2.4155(7)	2.4154(7)	2.4147(7)	2.4124(6)	2.4126(6)	2.4135(6)	2.4115(6)
Ca-O2	2.4475(6)	2.4483(7)	2.4473(6)	2.4462(6)	2.4444(6)	2.4438(6)	2.4437(6)	2.4430(6)
Ca-O5	2.5238(6)	2.5243(7)	2.5235(7)	2.5234(6)	2.5221(6)	2.5226(6)	2.5237(6)	2.5222(6)
Ca-O3	2.6121(6)	2.6105(6)	2.6093(6)	2.6077(6)	2.6056(6)	2.6042(6)	2.6035(6)	2.6027(5)
Ca-O3′	2.6583(6)	2.6593(7)	2.6576(6)	2.6554(6)	2.6543(6)	2.6532(6)	2.6530(6)	2.6510(5)
Ca-O5′	2.6705(6)	2.6716(7)	2.6705(7)	2.6695(7)	2.6668(6)	2.6667(6)	2.6656(6)	2.6651(6)
<Ca-O>	2.4856	2.4859	2.4849	2.4842	2.4825	2.4823	2.4821	2.4811
O1-Si-O2	113.83(3)	113.86(3)	113.87(3)	113.86(3)	114.00(3)	113.95(3)	113.98(3)	114.01(3)
O1-Si-O3	115.26(3)	115.32(3)	115.32(3)	115.33(3)	115.34(3)	115.36(3)	115.42(3)	115.40(3)
O1-Si-O4	108.77(3)	108.72(3)	108.76(3)	108.73(3)	108.63(3)	108.68(3)	108.62(3)	108.63(3)
O2-Si-O3	106.73(3)	106.70(3)	106.70(3)	106.65(3)	106.60(3)	106.61(3)	106.60(3)	106.58(3)
O2-Si-O4	106.19(3)	106.17(3)	106.13(3)	106.18(3)	106.19(3)	106.20(3)	106.17(3)	106.20(3)
O3-Si-O4	105.39(3)	105.38(3)	105.35(3)	105.40(3)	105.36(3)	105.33(3)	105.34(3)	105.32(3)
O2-B-O4	109.05(6)	109.01(7)	109.00(7)	109.00(7)	108.90(6)	109.06(6)	108.95(6)	109.09(6)
O2-B-O3	108.00(6)	107.94(7)	107.90(6)	108.02(6)	107.94(6)	107.85(6)	107.95(6)	107.86(6)
O2-B-O5	111.04(6)	110.95(7)	111.01(7)	111.05(7)	110.96(6)	110.99(6)	111.00(6)	111.10(6)
O3-B-O5	109.49(6)	109.47(7)	109.53(7)	109.50(6)	109.50(6)	109.49(6)	109.52(6)	109.42(6)
O3-B-O4	107.28(6)	107.43(7)	107.34(7)	107.34(7)	107.50(6)	107.39(6)	107.44(6)	107.32(6)
O4-B-O5	111.84(6)	111.90(7)	111.92(6)	111.79(6)	111.90(6)	111.92(6)	111.85(6)	111.91(6)
O5-H	0.813(16)	0.788(19)	0.783(19)	0.744(17)	0.799(16)	0.818(17)	0.819(16)	0.820(16)
O5···O4	2.993(1)	2.991(1)	2.992(1)	2.991(1)	2.991(1)	2.991(1)	2.990(1)	2.991(1)
H···O4	2.327(16)	2.371(20)	2.369(19)	2.416(18)	2.349(16)	2.310(17)	2.333(16)	2.321(17)
O5-H···O4	139.6(15)	136.3(19)	137.3(18)	135.4(17)	138.1(15)	141.1(16)	137.6(15)	139.4(15)
O5···O2	2.963(1)	2.962(1)	2.961(1)	2.960(1)	2.959(1)	2.960(1)	2.959(1)	2.958(1)
H···O2	2.364(15)	2.363(17)	2.371(17)	2.391(16)	2.384(14)	2.348(15)	2.359(14)	2.346(15)
O5-H···O2	131.2(13)	133.5(16)	133.0(16)	134.5(15)	129.8(13)	132.3(14)	130.7(13)	132.0(14)

~ 131° (Fig. 3; Tables 4 and 5[1]). These structural features are maintained within the *T*-range investigated. The high-quality low-*T* structure refinements show a monotonic trend in the evolution of the thermal displacement parameters of Ca, Si, B, and O sites vs. *T*. Figure 4 shows the evolution of *T* with the thermal parameters U_{eq} of the cation sites.

DISCUSSION AND CONCLUSIONS

This is the first comprehensive study of the crystal structure and crystal chemistry of a series of datolites from different localities and on the low-temperature structural evolution of this mineral, based on single-crystal X-ray diffraction and EPMA-WDS analysis. The chemical analyses show that all of the samples of investigated datolite have no significant site substitution (Table 1). The trace substitutions described in the work by Zaccarini et al. (2008), for the same set of crystals, could not be directly determined. A low amount of Na and Fe (i.e., ~0.01 apfu), as interlayer cations, was determined for other natural datolites (Ivanov and Belokoneva 2007).

Our single-crystal structure refinements confirm the overall structural model of datolite previously reported by Foit et al. (1973). Accordingly, the Si-tetrahedron is significantly distorted [with $\Delta(\text{Si-O})_{max}$ ~ 0.09 Å and $\Delta(\text{O-Si-O})_{max}$ ~ 10°; Tables 4 and 5[1]], the B-tetrahedron is almost regular [with $\Delta(\text{B-O})_{max}$ ~ 0.02 Å and $\Delta(\text{O-B-O})_{max}$ ~ 4°, Tables 4 and 5[1]], and the Ca-polyhedron is strongly deformed [with $\Delta(\text{Ca-O})_{max}$ ~ 0.4 Å, assuming CN = 8; Tables 4 and 5[1]]. The shortest Si-O bond distances occur with the "non-bridging" O1 oxygen (Fig. 1; Tables 4 and 5[1]). All the structure refinements of the different datolites investigated in this study show similar results. The consistency between the structural data reported here and those of Foit et al. (1973) and Ivanov and Belokoneva (2007) support the conclusions previously advanced about the nature of the chemical bonds in datolite by Hückel molecular orbital calculation (Foit et al. 1973), Hansen-Coppens multipole models, and Bader's topological analysis of the electron density (Ivanov and Belokoneva 2007; Gibbs et al. 2008), i.e., datolite possesses closed-shell type interactions between Ca and O atoms, whereas an intermediate nature with a significantly strong covalent component occurs in the intra-tetrahedral Si-O and B-O bonds.

Our structure refinements suggest a fully ordered Si/B-distribution, in agreement with the previous experimental findings (Foit et al. 1973; Ivanov and Belokoneva 2007). A disordered Si/B-distribution was observed in bakerite [$Ca_4B_5Si_3O_{15}(OH)_5$; Perchiazzi et al. 2004], a mineral with a marked structural analogy with datolite.

The high-quality structure refinements of this study allowed for the accurate location of the proton position and provide a consistent description of the hydrogen-bonding configuration. Only one independent H-site is observed with a bifurcated H-bonding scheme (with O5 as donor and O4 and O2 as acceptors; Fig. 3; Tables 4 and 5[1]). Such a configuration agrees with

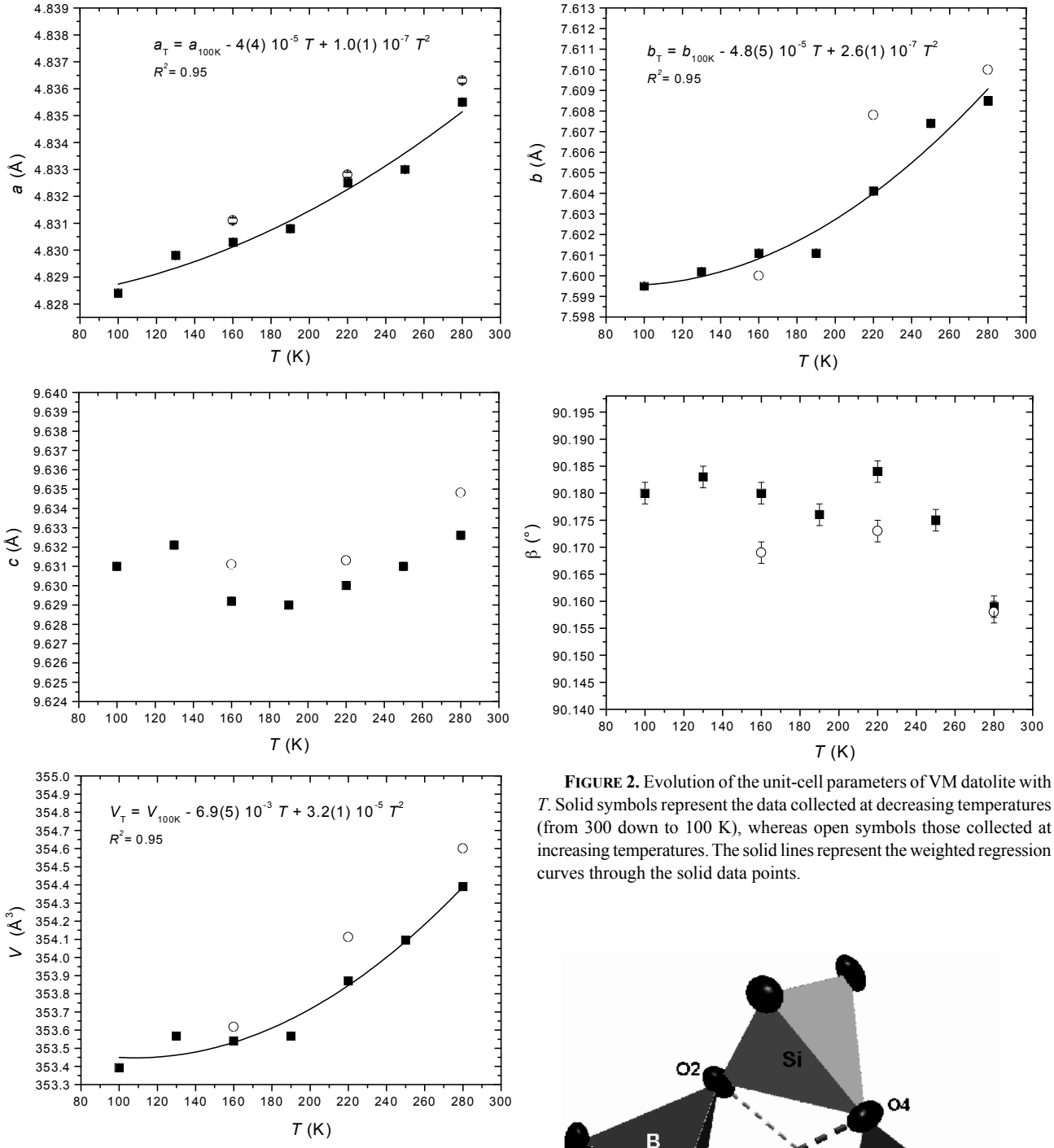

FIGURE 2. Evolution of the unit-cell parameters of VM datolite with *T*. Solid symbols represent the data collected at decreasing temperatures (from 300 down to 100 K), whereas open symbols those collected at increasing temperatures. The solid lines represent the weighted regression curves through the solid data points.

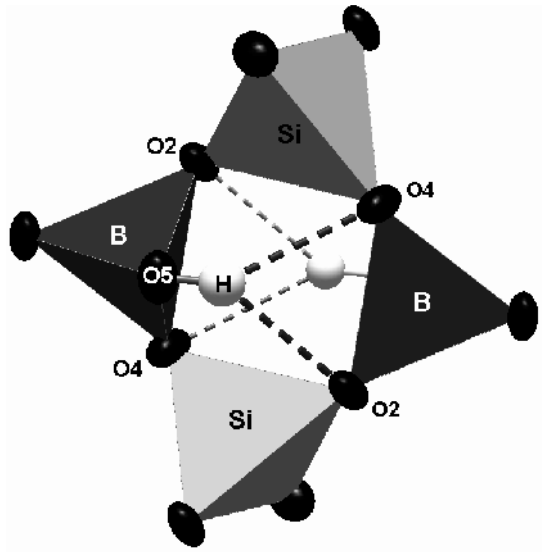

FIGURE 3. Hydrogen-bonding scheme in the datolite structure, with O5 as donor and O2 and O4 as acceptors.

the previous X-ray diffraction investigations (Foit et al. 1973; Ivanov and Belokoneva 2007), single-crystal proton magnetic resonance (Sugitani et al. 1972), and infrared pleochroism of the O-H stretching-frequencies in datolite (Sahl 1966). As expected from X-ray diffraction data [see for example data on hydrogarnet, Lager et al. (1987); micas, Ivaldi et al. (2001); epidotes, Comodi and Zanazzi (1997); Milman and Winkler (2001)], the O-H bond distance is slightly underestimated (i.e., O5-H ~ 0.8 Å, Tables 4 and 5[1]). Even a correction for the "riding motion effect," following the protocol of Busing and Levy (1964), leads to an increase of the O5-H distances of only 0.02–0.03 Å. The O5···O4 and

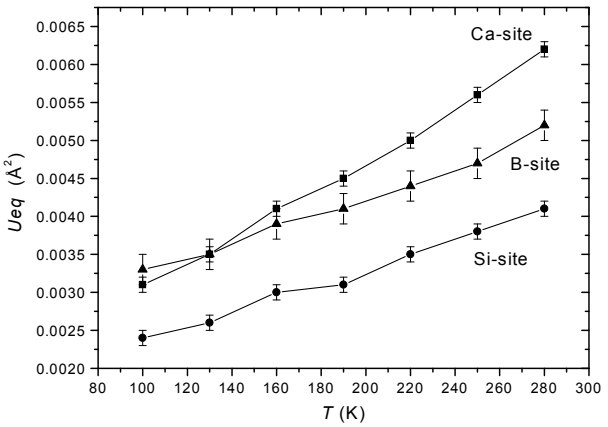

FIGURE 4. Evolution of the thermal displacement parameters (U_{eq}) of the Ca, Si, and B sites with temperature.

H···O4, as well as O5···O2 and H···O2 distances (Tables 4 and 5[1]), suggest a "moderate" hydrogen bond (sensu Gilli and Gilli 2009), with electrostatic-covalent nature.

ACKNOWLEDGMENTS

Our thanks go to Giorgio Garuti, Federica Zaccarini, and Maurizio Scacchetti for providing the five datolite samples from the Northern Italian Apennines, to Luca Bindi for the sample of Arendal datolite, and to Valeria Diella for her assistance with the electron probe microanalysis. Data collection at the Virginia Tech Crystallography Laboratory was made possible by the generous support of NSF grant EAR-0738692 to N.L. Ross and R.J. Angel, and the College of Science at Virginia Tech. G.D.G. acknowledges support from the University of Milan (PUR-2009). R.R. acknowledges support from the Italian Ministry of Foreign Affairs (MAE) for a travel grant to the U.S.A. within the Italy-U.S.A. cultural exchange program. Last but not least, the study would not have been possible without the logistic support provided to R.R. during his sabbatical visits, by Federica Zaccarini and Giorgio Garuti in Leoben, Austria, and Nancy Ross and Ross Angel in Blacksburg, Virginia. S.J. Mills, an anonymous reviewer, the technical editor R. Peterson, and associate editor H. Xu are thanked for their suggestions.

REFERENCES CITED

Bastin, G.F. and Heijligers, H.J.M. (1990) Quantitative electron probe microanalysis of ultralight elements (boron-oxygen). Scanning, 12, 225–236.

Bellatreccia, F., Càmara, F., and Della Ventura, G. (2006) Datolite: a new occurrence in volcanic ejecta (Pitigliano, Toscana, Italy) and crystal structure refinement. Rendiconti di Fisica dell'Accademia dei Lincei, 9–17, 289–298.

Busing, W.R. and Levy, H.A. (1964) The effect of thermal motion on the estimation of bond lengths from diffraction measurements. Acta Crystallographica, 17, 142–146.

Comodi, P. and Zanazzi, P.F. (1997) The pressure behaviour of clinozoisite and zoisite. An X-ray diffraction study. American Mineralogist, 82, 61–68.

Farrugia, L.J. (1999) WinGX suite for small-molecule single-crystal crystallography. Journal of Applied Crystallography, 32, 837–838.

Farsiyants, S.Yu., Opaleichuk, L.S., and Romanova, V.I. (1989) New types of filters. Glass and Ceramics, 46, 338–339.

Foit, F.F., Phillips, M.W., and Gibbs, G.V. (1973) A refinement of the crystal structure of datolite $CaBSiO_4(OH)$. American Mineralogist, 58, 909–914.

Gibbs, G.V., Downs, R.T., Cox, D.F., Ross, N.L., Prewitt, C.T., Rosso, K.M., Lippmann, Th., and Kirfel, A. (2008) Bonded interactions and crystal chemistry of minerals: a review. Zeitschrift für Kristallographie, 223, 1–40.

Gilli, G. and Gilli, P. (2009) The Nature of the Hydrogen Bond, p. 313. Oxford University Press, U.K.

Ivaldi, G., Ferraris, G., Curetti, N., and Compagnoni, R. (2001) Coexisting 3*T* and $2M_1$ polytypes of phengite from Cima Pal (Val Savenca, Western Alps): chemical and polytypic zoning and structural characterization. European Journal of Mineralogy, 13, 1025–1034.

Ivanov, Yu.V. and Belokoneva, E.L. (2007) Multiple refinement and electron density analysis in natural borosilicate datolite using X-ray diffraction data. Acta Crystallographica, B63, 49–55.

Ito, T. and Mori, H. (1953) The crystal structure of datolite. Acta Crystallographica, 6, 24–32.

Konerskaya, L.P., Orlova, R.G., Bogdanis, É.P., Konerskii, V.D., and Guseva, N.P. (1988) Using datolite and diopside raw materials in the electrical engineering industry. Glass and Ceramics, 45, 199–201.

Lager, G.A., Armbruster, T., and Faber, J. (1987) Neutron and X-ray diffraction study of hydrogarnet $Ca_3Al_2(O_4H_4)_3$. American Mineralogist, 72, 756–765.

Larson, A.C. (1967) Inclusion of secondary extinction in least-squares calculations. Acta Crystallographica, 23, 664–665.

Megaw, H.D. (1974) Tilts and tetrahedra in feldspars. In W.S. Mackenzie and J. Zussman, Eds., The Feldspars, p. 87–113. Manchester University Press, U.K.

Milman, V. and Winkler, B. (2001) Prediction of hydrogen positions in complex structures. Zeitschrift für Kristallographie, 216, 99–104

Olmi, F., Viti, C., Bindi, L., Bonazzi, P., and Menchetti, S. (2000) Second occurrence of okayamalite $Ca_2SiB_2O_7$: chemical and TEM characterization. American Mineralogist, 58, 1508–1511.

Ojovan, M.I. and Lee, W.E. (2005) An Introduction to Nuclear Waste Immobilisation, 315 p. Elsevier, Amsterdam.

Oxford Diffraction (2009) Xcalibur CCD system, CrysAlis Software system. Oxford Diffraction Ltd., Abingdon, Oxfordshire.

Pant, A.K. and Cruickshank, D.W.J. (1967) A reconsideration of the structure of datolite, $CaBSiO_4(OH)$. Zeitschrift für Kristallographie, 125, 286–297.

Paciorek, W.A., Meyer, M., and Chapuis, G. (1999) On the geometry of a modern imaging diffractometer. Acta Crystallographica, A55, 543–557.

Perchiazzi, N., Gualtieri, A.F., Merlino, S., and Kampf, A.R. (2004) The atomic structure of bakerite and its relationship to datolite. American Mineralogist, 89, 767–776.

Podlesov, V.V., Stolin, A.M., and Merzhanov, A.G. (1992) SHS extrusion of electrode materials and their application for electric-spark alloying of steel surfaces. Journal of Engineering, Physics and Thermophysics, 63, 1156–1165.

Rinaldi, R., Liang, L., and Schober, H. (2009) Neutron Applications in Earth, Energy and Environmental Sciences. In L. Liang, R. Rinaldi, and H. Schober, Eds., Neutron Applications in Earth, Energy and Environmental Sciences, p. 1–14. Springer, New York.

Sahl, K. (1966) Messung des Ultrarot-Pleochroismus von Mineralen. V. Der pleochroismus der OH Streckfrequenz in Datolit. Neues Jahrbuch für Mineralogie Monatshefte, 45–49.

Sheldrick, G.M. (1997) SHELX-97. Programs for crystal structure determination and refinement. University of Göttingen, Germany.

Schubert, D.M. (2003) Borates in industrial use. Structure and Bonding, 105, 1–40.

Sugitani, Y., Watanabe, M., and Nagashima, K. (1972) The positions of the hydrogen atoms in datolite as determined by nuclear magnetic resonance. Acta Crystallographica, B28, 326–327.

Tarasevich, B.P., Isaeva, L.B., Kuznetsov, E.V., and Zhenzhurist, I.A. (1991) Boron building ceramic protecting against neutron radiation. Glass and Ceramics, 47, 175–178.

Wilson, A.J.C. and Prince, E. (1999) International Tables for Crystallography Volume C. Kluwer, Dordrecht, The Netherlands.

Zaccarini, F., Morales-Ruano, S., Scacchetti, M., Garuti, G., and Heide, K. (2008) Investigation of datolite $CaBSiO_4(OH)$ from basalts in the Northern Apennines ophiolites (Italy): Genetic implications. Chemie der Erde, 68, 265–277.

MANUSCRIPT RECEIVED FEBRUARY 22, 2010
MANUSCRIPT ACCEPTED MAY 2, 2010
MANUSCRIPT HANDLED BY HONGWU XU